DNA Analysis

DOI: 10.1002/anie.200801304

Nanohybrid Carbon Film for Electrochemical Detection of SNPs without Hybridization or Labeling**

*Dai Kato, Naoyuki Sekioka, Akio Ueda, Ryoji Kurita, Shigeru Hirono, Koji Suzuki, and Osamu Niwa**

The rapid, simple, and low-cost detection of DNA is crucial to future genetic-disease diagnosis, such as the analysis of single-nucleotide polymorphisms (SNPs). With the development of many kinds of DNA analysis systems,[1,2] electrochemical techniques promise to meet the above requirements and also allow device miniaturization for samples with a very small volume. Several concepts for DNA electroanalysis have been reported including the direct oxidation of DNA, a hybridization-based technique with electroactive tags or intercalators, and an electron-transfer reaction through π-stacked DNA duplexes.[3–13] Of these, the direct oxidation of DNA is the simplest method.[7–13]

Electrodes made of carbon materials, such as glassy carbon (GC) and boron-doped diamond (BDD), have been widely used for such direct DNA measurements.[9–13] However, although the conventional GC electrode can detect guanine (G) and adenine (A) it cannot detect thymine (T) or cytosine (C), because the electrochemical potential window is narrow.[10,11] In addition, there is a large background current and the adsorption of oligonucleotides occurs after oxidation, which result in a reduction in both sensitivity and reproducibility.[11] By contrast, BDD is a suitable electrode material for the electroanalysis of DNA,[12,13] because BDD has a wide potential window, a low background current, and good biocompatibility.[12–14] These properties enable us to detect the four free bases by direct oxidation. However, it is difficult to conduct direct quantitative measurements of all the bases in oligonucleotides because of the relatively slow electron transfer at the BDD surface.[12,13]

In 2002, we described a nanocarbon film with a nanocrystalline sp^2 and sp^3 hybrid structure formed by employing the electron cyclotron resonance (ECR) sputtering method[15] (Figure 1a). This film has many advantages, such as high conductivity without doping and an atomically flat surface (Figure 1b,c), which provide excellent electrochemical characteristics including a wide potential window, a low background current, and little surface fouling by analytes after oxidation.[11,16] Most importantly, the sp^3/sp^2 ratio in the ECR nanocarbon film can be widely controlled by manipulating the sputtering conditions. These characteristics allow the detection of pyrimidine bases with slower electron-transfer rates, while maintaining a wide potential window and low background current. As a result, we succeeded in the direct quantitative measurement of DNA methylation, which enabled us to detect cytosine and methylcytosine individually, by using the ECR nanocarbon film electrode.[17] These film

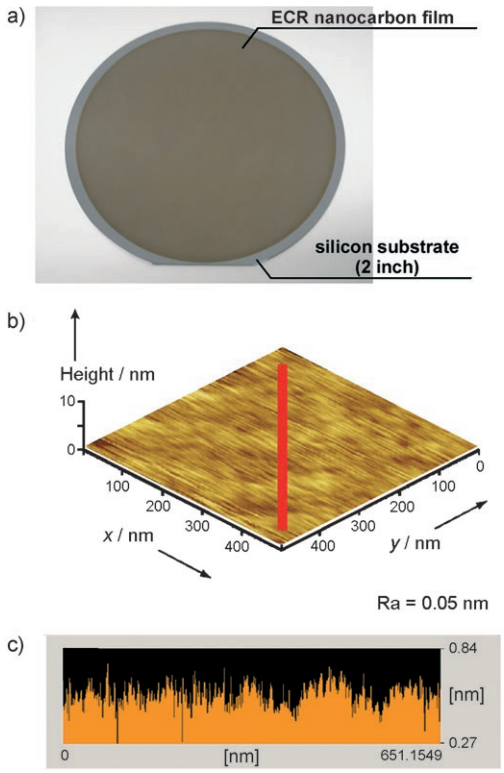

Figure 1. a) Photograph, b) AFM image, and c) line profile of the ECR nanocarbon film surface. A typical average roughness (Ra) of 0.05 nm was obtained for the film, determined by scanning along the red line in (b).

[*] Dr. D. Kato, Dr. R. Kurita, Prof. O. Niwa
National Institute of Advanced Industrial Science and Technology
1-1-1 Higashi, Tsukuba, Ibaraki 305-8566 (Japan)
Fax: (+81) 29-861-6177
E-mail: niwa.o@aist.go.jp
N. Sekioka, Prof. O. Niwa
Graduate School of Pure and Applied Sciences
University of Tsukuba, Ibaraki 305-8571 (Japan)
A. Ueda, Prof. O. Niwa
Interdisciplinary Graduate School of Science and Engineering
Tokyo Institute of Technology, Yokohama 226-8503 (Japan)
Dr. S. Hirono
MES-Afty Corporation, Tokyo 192-0918 (Japan)
Prof. K. Suzuki
Department of Applied Chemistry, Keio University (Japan)

[**] This work was supported by the CREST-JST project. SNP = single-nucleotide polymorphism.

Supporting information for this article is available on the WWW under http://dx.doi.org/10.1002/anie.200801304.

properties can be employed to realize the simple SNP detection needed to discriminate single-base differences solely by measuring the peak-current differences caused by a single-base mismatch. This is despite the fact that analysis is more difficult because all four bases are capable of associating with SNPs.

Herein, we used the ECR nanocarbon film electrode to develop the label-free electrochemical detection of SNPs of oligonucleotides, based on the direct oxidation of all the bases in both a wild-type oligonucleotide and its mismatch-type oligonucleotide. Figure 2 outlines the concept behind our

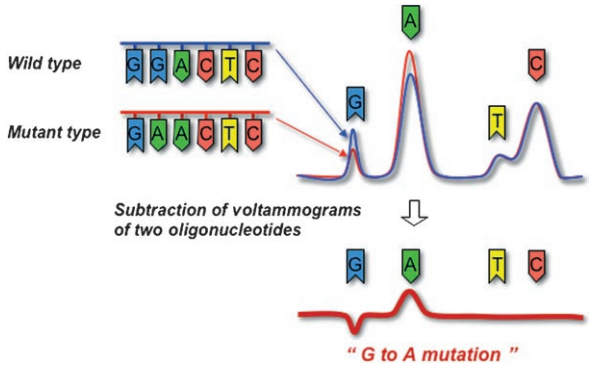

Figure 2. Proposed concept of electrochemical detection of SNPs for single-strand oligonucleotides.

SNP detection methodology. When we subtract the voltammograms obtained by the electrochemical oxidation of a wild-type oligonucleotide (5′-GGACTC-3′) and its single-base mismatch oligonucleotide (5′-GAACTC-3′; the underlined base represents a mismatch base), the result is a pair of positive and negative peak currents assigned to A and G, respectively. This indicates "G→A mutation" as shown in the subtracted curve. This method offers the simplest SNP analysis because no hybridization or labeling processes are needed. No such concept has yet appeared, despite reports of SNP analysis combined with a variety of analytical signals including electrochemical and fluorescence detection.[1–7]

Moreover, even if the concentrations of the wild- and mismatch-type oligonucleotides are different, this method can be used to detect the SNP between them by normalizing the peak currents of the nonmutational bases, as the total content of each base in the oligonucleotides can be quantitatively measured over a relatively wide concentration range. The remaining problem is that a very similar signal is obtained for oligonucleotides with the same base content but different contexts and this makes it difficult to detect SNPs. Nevertheless, we can use this method to detect an SNP site for short oligomers with a particular sequence without any hybridization or labeling processes.

We used an ECR nanocarbon film electrode with its electrochemical properties optimized by changing the ion acceleration voltage during sputtering and electrochemical pretreatment. The film with an $sp^2/(sp^2+sp^3)$ ratio of 0.6 had a sufficiently wide potential window with high electrode activity, and stability against fouling.[17] The ECR nanocarbon film electrode provided electrochemical responses for all the nucleotide monophosphates (NMPs) that were superior to those of GC or BDD electrodes, because the film electrode provided a wide potential window while maintaining high electrode activity (see the Supporting Information). The excellent properties of this film electrode result from its homogeneous and stable structure that consists solely of nanocrystalline sp^2 and sp^3 carbon hybrids, which induce high electrode activity against aromatic DNA bases as a result of π–π interaction.[17–19] This nanocrystalline structure is quite unlike those of GC and BDD electrodes,[17] and therefore is alone in achieving high electrode activity without losing the wide potential window needed for oxidizing uridine monophosphate, with the highest oxidation potential of all the bases (see the Supporting Information).

Figure 3 shows background-subtracted differential pulse voltammograms (DPVs) of an oligonucleotide based on a CAG repeating unit (**1**) and its base-mismatch oligonucleotides **2**–**4**. We could quantitatively differentiate the voltammograms for these oligonucleotides because the current responses coincided precisely with the base content of each oligonucleotide at the ECR nanocarbon electrode (Figure 3a). For example, when the DPV result for **1** is compared with that for single-base-substituted **2**, the peak current based on G was higher than that of **2**, whereas the peak current based on A was lower than that of **2**. These differences between the current heights of the two oligonucleotides can be unambiguously attributed to the corresponding base content of the oligonucleotides. Therefore, we could readily detect single G→A mutation without any current height change for C.

In the same way, the peaks for G and A from **1** were also assigned at the GC and BDD electrodes. However, in these measurements the oxidation of C was not observed at the GC electrode because of the large background current (Figure 3b), and a reproducible C oxidation current could not be obtained with the BDD electrode because of its low electrochemical activity (Figure 3c). This finding indicates that it is difficult to normalize a wild-type oligonucleotide and its single-base mismatch oligonucleotides with different concentrations. Furthermore, mutation detection with respect to pyrimidine bases, such as C→T or G→T mutations, should be more difficult to achieve with GC and BDD electrodes.

We employed the method to detect SNPs in sequences that are naturally occurring mutational hotspots from the p53 tumor suppressor gene.[5,20,21] The p53 gene, also known as "the guardian of the genome", encodes an important transcription factor that conserves stability by preventing genome mutation. Most tumor-inducing mutations have been observed in areas that encode the DNA-binding domain (in codons 100–293) and there are five main hotspots (codons 175, 245, 248, 249, and 273).[20,21] We performed the direct detection of two kinds of mutation in codon 248 of the p53 gene frequently observed in various types of cancer.[20,21]

Figure 4 shows the background-subtracted square-wave voltammograms (SWVs) of a wild-type oligonucleotide **5** and its single-base mismatch oligonucleotides **6** and **7** including the sequence from codon 248 of the p53 gene. The G→A mutation could be clearly distinguished from the difference between the voltammograms of **5** and **6** (Figure 4a).

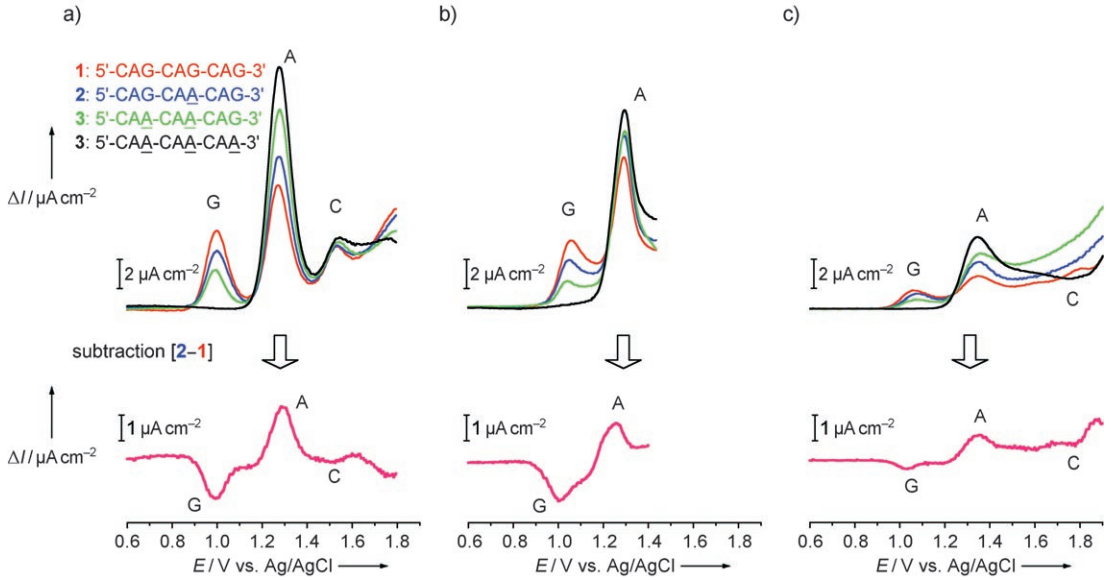

Figure 3. Electrochemical responses of oligonucleotides. Background-subtracted DPVs of oligonucleotide **1** (3 μM) and its base-mismatch oligonucleotides **2**–**4**, and the subtraction of the DPVs of **1** and **2** at a) ECR nanocarbon film, b) GC, and c) BDD electrodes, respectively, measured in acetate buffer (50 mM, pH 5.0).

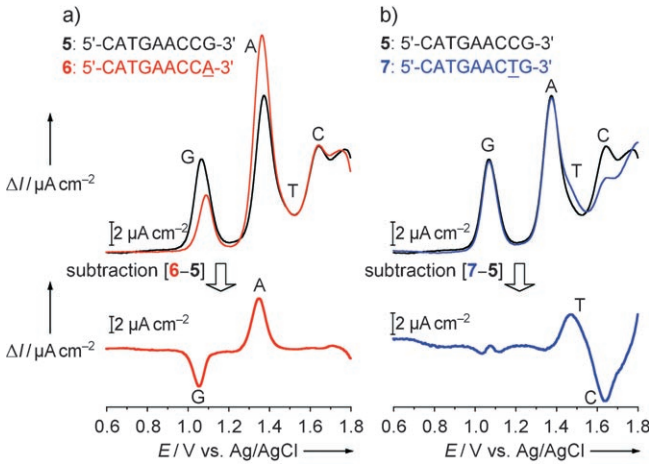

Figure 4. Detection of SNPs of oligonucleotides including the sequence from codon 248 of the p53 gene by using the ECR nanocarbon film electrode. a) Background-subtracted SWVs of wild-type oligonucleotide **5** (1 μM) and its single-base mismatch **6**, and the subtraction of the SWVs of **5** and **6** (G→A mutation). b) Background-subtracted SWVs of wild-type **5** (1 μM) and its single-base mismatch **7** and the subtraction of the SWVs of **5** and **7** (C→T mutation). All SWVs were measured in acetate buffer (50 mM, pH 3.3) containing 2 M sodium nitrate.

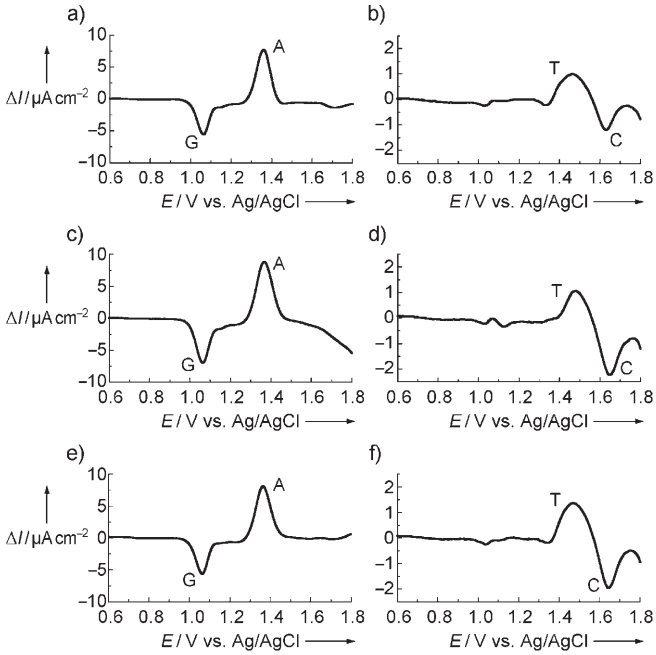

Figure 5. SNP detection in combinations of different concentrations of two oligonucleotide samples by using the ECR nanocarbon film electrode. Subtractions of the SWVs of a) **5** (5 μM) and **6** (3 μM), b) **5** (1 μM) and **7** (2 μM), c) **5** (10 μM) and **6** (8 μM), d) **5** (2 μM) and **7** (3 μM), e) **5** (5 μM) and **6** (4 μM), and f) **5** (2 μM) and **7** (4 μM) were obtained by normalizing the peak currents of the nonmutational bases C and A of **5**, respectively, measured in acetate buffer (50 mM, pH 3.3) containing 2 M sodium nitrate.

As regards to the C→T mutation, the T and C peaks obtained from the SWV measurements of **5** and **7** overlapped even when using the ECR nanocarbon film electrode. However, the subtraction of the two voltammograms led to a clearer discrimination of C→T mutation (Figure 4b).

Moreover, we demonstrated how effectively peak current normalization works for two different sequences. Figure 5 shows the subtractions of SWVs of **5** and **6** and of **5** and **7** with different concentrations by normalizing the peak currents of the nonmutational bases C and A of **5**, respectively. This normalization works well and provides clear mutation detection effectively over a relatively wide concentration range as good as that in Figure 4, which was achieved by using samples with the same concentration. Relative standard deviations of the peak-area ratios (G/A and T/C) obtained

from Figure 5 were 1.5 and 3.3 % ($n = 3$), respectively. This is because the ECR nanocarbon electrode can quantitatively measure the total content of each base in the oligonucleotides.

In contrast, such a normalization was impossible on GC and BDD electrodes. If there are extreme differences between the concentrations of the two samples, diluted standard samples with different concentrations should be prepared, similar to the technique used to obtain calibration curves. We also obtained detection limits of 125 fmoles for G and A in **5**, and 6.25 pmoles for **5** itself (signal-to-noise ratio = 3, volume = 5 μL). As regards reproducible measurement, the ECR nanocarbon electrode provided the most stable results for the entire base content of oligonucleotide **1**, despite a gradual decrease in the peak currents. In contrast, the other electrodes did not exhibit a stable result, particularly in the case of C in **1** (see the Supporting Information).

In conclusion, we successfully used an ECR nanocarbon film electrode to develop a simple electrochemical analysis technique for SNPs without hybridization, labeling processes, or the use of electrochemical mediators or indicators. We will develop this approach to achieve a more sophisticated SNP electroanalysis technique with a view to extending it to various sequences, including longer DNA fragments, by using a combination of enzymatic or separation technologies.

Received: March 18, 2008
Revised: June 6, 2008
Published online: July 21, 2008

Keywords: carbon electrodes · electrochemistry · oligonucleotides · oxidation · polymorphism

[1] M. Strerath, A. Marx, *Angew. Chem.* **2005**, *117*, 8052 – 8060; *Angew. Chem. Int. Ed.* **2005**, *44*, 7842 – 7849.
[2] A. Sassolas, B. D. Leca-Bouvier, L. J. Blum, *Chem. Rev.* **2008**, *108*, 109 – 139.
[3] F. Patolsky, Y. Weizmann, I. Willner, *J. Am. Chem. Soc.* **2002**, *124*, 770 – 772.
[4] F. Patolsky, E. Katz, I. Willner, *Angew. Chem.* **2002**, *114*, 3548 – 3552; *Angew. Chem. Int. Ed.* **2002**, *41*, 3398 – 3402.
[5] E. M. Boon, D. M. Ceres, T. G. Drummond, M. G. Hill, J. K. Barton, *Nat. Biotechnol.* **2000**, *18*, 1096 – 1100.
[6] K. Kerman, M. Kobayashi, E. Tamiya, *Meas. Sci. Technol.* **2004**, *15*, R1 – R11.
[7] T. G. Drummond, M. G. Hill, J. K. Barton, *Nat. Biotechnol.* **2003**, *21*, 1192 – 1199.
[8] E. Palecek, *Nature* **1960**, *188*, 656 – 657.
[9] J. Wang, S. Bollo, J. L. L. Paz, E. Sahlin, B. Mukherjee, *Anal. Chem.* **1999**, *71*, 1910 – 1913.
[10] A. M. O. Brett, J. A. P. Piedade, L. A. Silva, V. C. Diculescu, *Anal. Biochem.* **2004**, *332*, 321 – 329.
[11] O. Niwa, J. B. Jia, Y. Sato, D. Kato, R. Kurita, K. Maruyama, K. Suzuki, S. Hirono, *J. Am. Chem. Soc.* **2006**, *128*, 7144 – 7145.
[12] T. A. Ivandini, B. V. Sarada, T. N. Rao, A. Fujishima, *Analyst* **2003**, *128*, 924 – 929.
[13] C. Prado, G. U. Flechsig, P. Grundler, J. S. Foord, F. Marken, R. G. Compton, *Analyst* **2002**, *127*, 329 – 332.
[14] W. S. Yang et al., *Nat. Mater.* **2002**, *1*, 253 – 257.
[15] S. Hirono, S. Umemura, R. Kaneko, *Appl. Phys. Lett.* **2002**, *80*, 425 – 427.
[16] J. B. Jia, D. Kato, R. Kurita, Y. Sato, K. Maruyama, K. Suzuki, S. Hirono, T. Ando, O. Niwa, *Anal. Chem.* **2007**, *79*, 98 – 105.
[17] D. Kato, N. Sekioka, A. Ueda, R. Kurita, S. Hirono, K. Suzuki, O. Niwa, *J. Am. Chem. Soc.* **2008**, *130*, 3716 – 3717.
[18] J. A. Bennett, J. A. Wang, Y. Show, G. M. Swain, *J. Electrochem. Soc.* **2004**, *151*, E306 – E313.
[19] P. H. Chen, R. L. McCreery, *Anal. Chem.* **1996**, *68*, 3958 – 3965.
[20] T. Soussi, J. M. Rubio-Nevado, D. Hamroun, C. Béroud in *The p53 Mutation Handbook*, **2007** (http://p53.free.fr/index.html).
[21] M. Hollstein, D. Sidransky, B. Vogelstein, C. C. Harris, *Science* **1991**, *253*, 49 – 53.

